

Reactive flash sintering: MgO and α -Al₂O₃ transform and sinter into single-phase polycrystals of MgAl₂O₄

Bola Yoon¹  | Devinder Yadav¹ | Sanjit Ghose²  | Rishi Raj¹ 

¹Materials Science and Engineering Program, Department of Mechanical Engineering, University of Colorado Boulder, Boulder, Colorado

²Energy Sciences Directorate/Photon Science Division, NSLS II, Brookhaven National Laboratory, Upton, New York

Correspondence: Rishi Raj, Materials Science and Engineering Program, Department of Mechanical Engineering, University of Colorado Boulder, Boulder, CO 80309-0427 (rishi.raj@colorado.edu).

Funding information

DOE Office of Science, Grant/Award Number: DE-SC0012704; Office of Science of the Department of Energy, Grant/Award Number: DE-AC02-98CH10886; Army Research Office, Grant/Award Number: W911NF-16-1-0200; US Department of Energy

Abstract

We show that flash experiments with three phase mixed-powders of yttria-stabilized zirconia (8YSZ), MgO, and α -Al₂O₃ not only produce polycrystals of high density, but also the transformation of magnesia and alumina into single-phase spinel. The presence of zirconia facilitates the onset of the flash. The sintering experiments in the laboratory were extended to live experiments at the National Synchrotron Light Source II at Brookhaven National Laboratory in order to measure the time-dependent evolution of single-phase spinel. The phase transformation occurred in <3 seconds during Stage II. Later, during Stage III the cubic zirconia transformed partly into the monoclinic phase, which reverted back to the cubic phase when the flash was extinguished by turning off the current to the specimen. The results underpin a recent report on the synthesis of single-phase bismuth ferrite from constituent oxides in reactive flash experiments, raising the specter of flash as a method for synthesis as well as sintering of complex oxide ceramics. The role of zirconia in catalyzing the flash in the present study is discussed.

1 | INTRODUCTION

Flash sintering was first reported in 2010, where 3 mol% stabilized zirconia (3YSZ) was shown to sinter in <5 seconds at a furnace temperature of 850°C at field of 120 V/cm.¹ Since then the method has been shown to apply to various ceramic materials, including, among others, titania (TiO₂),² yttria (Y₂O₃),³ Mg-doped alumina (Al₂O₃),⁴ zinc oxide (ZnO),⁵ and magnesium aluminate spinel (MgAl₂O₄).⁶

Very recently, the technique has been extended to reactive flash sintering whereby flash induces both phase transformation and sintering, simultaneously. Gil-Gonzalez et al⁷ have fabricated dense, phase-pure polycrystals of BiFeO₃, from powders of Bi₂O₃ and Fe₂O₃ in a one-step flash experiment.

The experiments presented here further underpin the results just above,⁷ providing growing evidence that single-phase oxides of complex compositions can be produced from their simple constituents.

In situ experiments at X-ray synchrotrons can measure time-dependent evolution of the field-induced phases. For example, experiments at APS (Argonne National Laboratory) have shown the development of a far-from-equilibrium phase during flash sintering of 3YSZ, which was shown to emerge and then extinguish repeatedly when the electrical field to the specimen was turned on and off.⁸ Flash sintering of titania exhibited time-dependent fluctuation in texture during these live experiments.⁹ Alumina and titania were shown to react to form single-phase titanate at anomalously high rates.¹⁰

Evidence for the formation of phases far from equilibrium in flash experiments, continues to grow. For example, very recently, Kok et al¹¹ have shown the evolution of a high alumina phase of spinel, which is outside the equilibrium regime of the phase diagram; this reaction was shown to occur within 2 or 3 seconds.¹²

In this study, we consider experiments of reactive flash sintering applied to the production of single-phase spinel

from powders of alumina and spinel according to the following reaction



Laboratory results are followed up with live experiments at NSLS-II (Brookhaven National Laboratory) to measure the rate of this reaction.

The present work is unique in one other respect. The experiments are carried out with mixtures of three powders, magnesia, alumina, and zirconia. Stand alone experiments with single phases have shown that magnesia and pure alumina do not flash at least up to fields of 1000 V/cm and temperatures of up to 1300°C, while zirconia can be flashed below 1000°C at fields of about 100 V/cm. Here, we find a catalytic effect of zirconia on the flash of the three-phase powders. We show that the effect depends on the volume fraction of the zirconia powder.

The flash experiments at our Boulder laboratory were carried out, as in the original work,¹ by applying a field and heating the specimen at a constant heating rate until flash and then switching to current control. The synchrotron experiments were conducted at isothermal furnace temperature; a voltage was applied as a step function, and the power supply was switched to a preset current limit at the onset of the flash.¹³

2 | EXPERIMENTAL: MATERIALS AND METHODS

2.1 | Laboratory experiments

Powder mixture consisted of various volume fractions (20, 30, 40, and 50 vol%) of yttria (8 mol%) stabilized zirconia (TZ-8Y, Tosoh USA, Grove City, OH), Al₂O₃ (Taimicron TMDAR, Taimei Chemical Co., Ltd., Tokyo, Japan) and MgO (99.9%; Inframat Advanced Materials, Manchester, CT). The relative amounts of MgO and Al₂O₃ were chosen to be equal to the composition of MgAl₂O₄. Average particle size of 8YSZ, Al₂O₃, and MgO were 25 nm, 0.5 μm, and 1 μm, respectively. The powder mixture was ball milled in deionized water with 5 wt% binder (Duramax B-1000; Rohm and Haas, Philadelphia, PA) and zirconia balls for 2 hours and dried in 90°C oven. The dried powders were ground and cold-pressed into dies for both laboratory and the synchrotron experiments. For the laboratory experiments, the dog-bone shaped specimens had a gauge length of 15 mm, width of 3.5 mm, and thickness of 1.5 mm. The samples were heated at 2°C/min up to 600°C and held there for 1 hour to burn out the binder. The green densities of the samples were in a range of 50%-55%.

For a baseline, samples were also prepared by conventional sintering of the same powder mixture. This procedure was carried out at 1550°C for 2 hours in air.

Flash sintering experiments were performed using a 3000W DC power supply (Glassman High Voltage, Inc., Whitehouse Station, NJ). The current was recorded with a Keithley multimeter model 2000 (Keithley Instruments, Cleveland, OH). Sample was suspended in the center of horizontal furnace by Kanthal wires. Both sides of sample were pasted with thin platinum for a good electrical contact.

The laboratory experiments were carried out by heating the furnace at a rate of 10°C/min. The current limit was set to 60 mA/mm². A CCD camera with optical filters recorded the sample dimensions to measure linear shrinkage. The shrinkage strain was measured from $\varepsilon = \ln(L/L_0)$, where L_0 is the original gauge length and L is the time dependent length. The density, ρ , was calculated from shrinkage data, using $3\varepsilon = \ln(\rho_g/\rho)$, where ρ_g is the green density. Relative densities of the flash sintered specimens are listed in Table 1.

The sintered specimen was metallographically polished and thermally etched at 1150°C for 1 hour. The morphology of the samples was analyzed using a scanning electron microscope (SEM, SU-3500; Hitachi, Tokyo, Japan). Average grain size was measured by linear intercept method.

2.2 | In situ synchrotron X-ray diffraction experiments

Synchrotron X-ray diffraction experiments were carried out at the beamline XPD 28ID-2 of the National Synchrotron Light Source II (NSLS II) at Brookhaven National Laboratory using a wavelength $\lambda = 0.1867 \text{ \AA}$ (66.408 keV).¹⁴ The experimental setup for this study has been described previously.¹⁵ Briefly, the powder mixture was cold pressed under 100 MPa to rectangular bars, which have dimensions of 6 mm × 1.6 mm × 0.8 mm. The samples were pre-sintered at 900°C for 1 hour. A DC power source (Sorenson 300-2; Sorenson, San Diego, CA) and a digital multimeter (Keithley 2000; Keithley Instruments) were used for flash experiments. The samples were wrapped in platinum wires, held within an alumina holder, and placed in the hot zone of a quadrupole lamp furnace. Final gauge length of the samples was 4 mm. The flash experiment was carried out at a furnace temperature set at 900°C.

TABLE 1 Relative densities of flash and conventionally sintered samples

Electric field (V/cm)	Current density (mA/mm ²)	Relative density (%)
300	60	93.0
500	60	93.4
750	60	99.5
1000	60	97.3
Conventionally sintered density = 91%		

Fit2D software was used to obtain one-dimensional powder diffraction patterns from raw two-dimensional patterns.¹⁶ Platinum standard was used for measuring the specimen temperature. For this purpose, a thin line of platinum was applied on surface of the sample. Shifts in the (111) and (200) peaks of platinum were analyzed while the specimen was heated up to 1500°C without the electric field, and sample temperature was calibrated using thermal expansion data for platinum.¹⁷ This calibration curve was used to measure the specimen temperature during the flash experiments.

Sample temperature was also estimated from the black body radiation (BBR) model, where

$$T/T_0 = \left[1 + \frac{1000W_v}{\varepsilon\sigma T_0^4} \left(\frac{V}{A} \right) \right]^{\frac{1}{4}} \quad (2)$$

Here, W_v is the power dissipation in the sample, in units of mW/mm³, V/A is volume to surface area ratio, expressed in units of mm, $\sigma = 5.67 \times 10^{-8}$ W/m²/K⁴ which is the Stefan-Boltzmann constant. ε is emissivity. The BBR estimate was compared with temperature obtained from the platinum standard.

The diffraction peak was fitted using *pseudo-voigt equation* written in Matlab, which can measure peak position, intensity, and area. We repeated the analysis 15 times for accuracy.

3 | RESULTS

The results are divided into three main sections. The first section presents results from the experiments carried out in our laboratory in Boulder.

The second section presents results that correlate the electrical response to the evolution of the spinel phase from magnesia and alumina.

In the third section, we present a critical assessment of the live measurements of the specimen temperature, as measured at NSLS-II with the platinum standard, which are compared with the estimates from the BBR model according to Equation (2).

3.1 | Influence of flash parameters on sintering and microstructure

Flash sintering experiments were carried out at constant heating rate of 10°C/min. Four levels of electrical fields, 300, 500, 750, and 1000 V/cm were considered. The onset of the flash was signaled by an abrupt rise in the conductivity of the specimen. The results for 50 vol% of 8YSZ are shown in Figure 1. The flash temperature falls from 950°C at 300 V/cm, to 730°C at 1000 V/cm.

Arrhenius plots of power dissipation are shown in Figure 2. Flash is signaled by the abrupt increase in the power

dissipation. For comparison the flash behavior of pure 8YSZ is also included. Note that at 500 V/cm the 50 vol% 8YSZ composite flashes at 820°C, while 100% 8YSZ flashes at 621°C. Further results for lower volume fractions of 8YSZ in the powder mixtures are given in Figure 3. Note that the flash for the composite moves to even higher temperature as the volume fraction of 8YSZ is reduced, until the flash does not occur when the volume fraction is <20%.

It is important to note that the power density at the cusp of flash onset in Figure 3, regardless of the volume fraction of 8YSZ lies within a narrow range of 10-30 mW/mm³. Furthermore, the same range of power density holds for flash in 50 vol% specimens, in Figure 2. The power dissipation in the specimen is given by $E^2\sigma$ where E is the applied field and σ is the conductivity of the specimen. The interplay of the field and the conductivity on the flash onset can be discerned from the results in Figures 2 and 3, keeping in mind that the conductivity increases Arrheniusly with temperature.

First consider Figure 3. Here, the field is held constant while the composition of the composite is changed by adding different amounts of 8YSZ. In the mixture, 8YSZ is the conducting phase while both magnesia and alumina are insulating. Therefore, increasing the amount of 8YSZ increases the conductivity of the composite, allowing $E^2\sigma$ to reach a given value at a lower temperature, if E is held constant. When the volume fraction of 8YSZ falls below 20 vol%, the conductivity is too low to reach the required value of power dissipation.

The same behavior is present in Figure 2. Here, the composition of the mixture is held constant. As the field is increased, $E^2\sigma$ reaches the threshold at a lower conductivity.

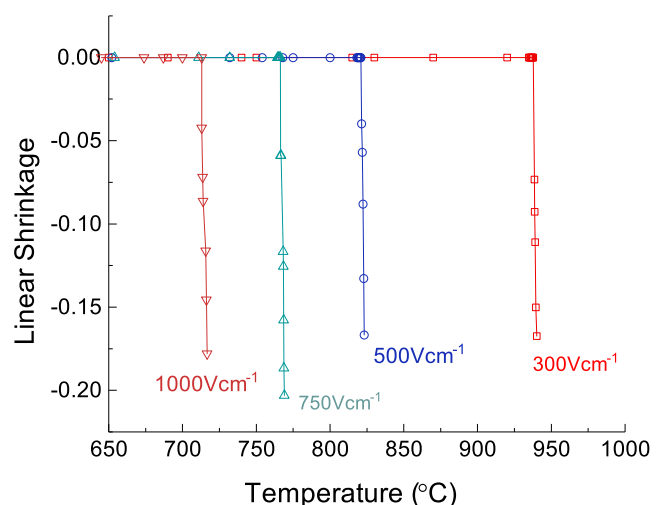


FIGURE 1 Linear shrinkage curves at different electric field with current density limit of 60 mA/mm² [Color figure can be viewed at wileyonlinelibrary.com]

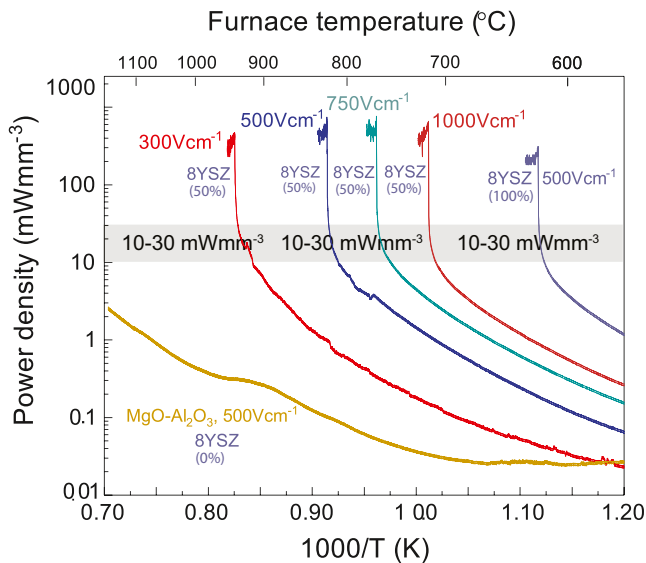


FIGURE 2 Arrhenius plots of power dissipation of composite and single phase 8YSZ at different electric fields [Color figure can be viewed at wileyonlinelibrary.com]

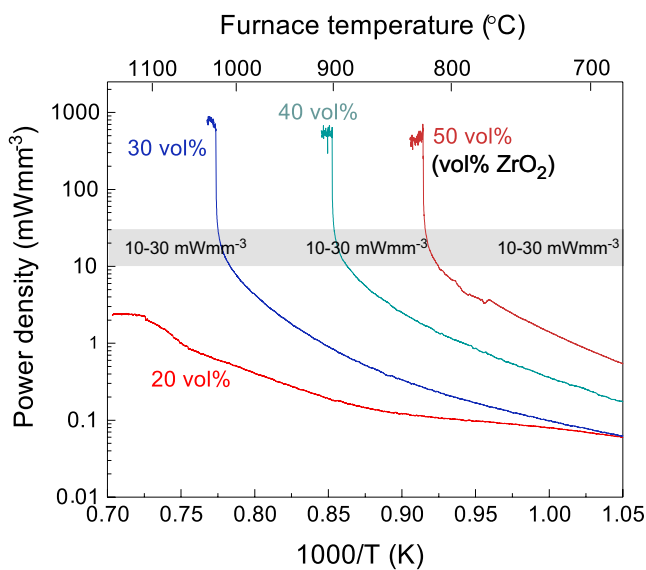


FIGURE 3 Arrhenius plots of power dissipation of composites with different volume fractions of 8YSZ under an electric field of 500 V/cm [Color figure can be viewed at wileyonlinelibrary.com]

It may be inferred that the MgO-Al₂O₃ composite, without the addition of zirconia, failed to flash because its conductivity was too low to reach the threshold value of 10–50 mW/mm³, and that zirconia catalyzes the flash simply by increasing the electrical conductivity of the composite.

3.2 | Microstructure

In this section, we compare the microstructure of conventionally sintered specimens with those prepared by reactive flash sintering.

From the literature conventional reactive sintering of spinel with mixed powders of magnesia and alumina is carried out in two steps: holding at 1300°C for 4 hours at which point 90% of the reaction is complete, followed by sintering above 1600°C for more than 2 hours.¹⁹ In the present work the reaction and sintering were carried out in one-step, by heating the powder mixtures at 1550°C for 2 hours. This method yielded a density of 91%. X-ray diffraction of this specimen revealed no residual phase of magnesia and alumina.

The microstructures of the conventionally and flash sintered samples are shown in Figure 4. The dark and bright phase corresponds to spinel and zirconia, respectively. The conventionally sintered sample shows a large grain size about 0.63 μm. The grain size of the flash sintered sample is smaller, and decreases with higher electric field. This result is similar to previous studies on MgAl₂O₄, 3YSZ, and 3YSZ-Al₂O₃ composite. Yoshida et al⁶ have reported that flash sintering of spinel showed smaller grain size than conventional sintering (5 μm vs 80 μm). Naik et al²⁰ have shown that grain size of 3YSZ-Al₂O₃ composite decreased with increasing field. A study of 3YSZ showed high population densities of nano-scale grains.²¹ Note that the sample in Figure 4C, sintered with 1000 V/cm consists of significant areas where the grain size is nanoscale. The present results show smaller grain size than in previous study on MgAl₂O₄,⁶ which reported the average grain size 5 μm using initial particle size of 250 nm. The finer grain size in the present work may have resulted because the addition of zirconia lowered the flash temperature relative to experiments with pure spinel.⁶

3.3 | In situ experiments at NSLS II

The purpose of these experiments was to determine the time scale for the evolution of the spinel phase. Isothermal experiments where the specimen is held at a constant temperature, and the field is applied as a step function were more appropriate for this determination since these experiments are distinctly separated into three Stages. The first stage is an incubation time before the onset of the flash, then Stage II is when the sudden rise in conductivity is controlled by switching the power supply from voltage to current control, and finally, Stage III, when the specimen can be held in a constant state of flash under current control. In previous work, it has been shown that sintering occurs during the short-lived period of Stage II, lasting <5 seconds.¹³

The results presented below are separated into two parts. The first shows the transformation of magnesia and alumina into single-phase spinel, which occurs quickly during Stage II. However, as the specimen is held in Stage III over a longer period, the cubic phase of zirconia transforms

into the (non-equilibrium) monoclinic phase, which reverts to the cubic phase when the electric current is switched off.

These experiments were carried out at a furnace temperature of 975°C. The initial applied field was 600 V/cm. The current limit was set to 60 mA/mm². The three stages of the flash experiments are shown in Figure 5.

The time-dependent change in the diffraction peaks for alumina, magnesia, spinel are given in Figure 6, and those for zirconia in Figure 7.

The transformation of magnesia and alumina into spinel is clearly seen in Figure 6. The two phases remain distinct during Stage I, before the onset of the flash; these data are marked by points #1, #2, and #3, in Figure 5B. The transformation to spinel is nearly complete during Stage II marked by points #4 and #5 in Figure 5B. Point #4 is near the power peak while #5 is just after the current control is established; these two points span Stage II. The transformation is nearly complete at #4, that is, within a few seconds. However, small residual alumina and magnesia peaks remain which gradually dissolve into spinel during Stage III.

The change in the zirconia peaks are shown in Figure 7. Note the evolution of new diffraction peaks late in Stage III (corresponding to points #7 and #8 in Figure 5), near 4° and 6.6°. These new peaks could be indexed to monoclinic zirconia (002) and (031) plane (JCPDS 83-0944). Detailed peak analysis was carried out for cubic zirconia (111) and monoclinic (002) peaks. Time dependent change in the diffraction peaks for zirconia can be observed in the Video S1. The data, synchronized with the power density, are shown in the plots in Figure 8. The (111) peak from the cubic phase and the (002) peak from the monoclinic phase of zirconia are shown. We plot the areas under the peaks since that is representative of the mole fraction of the phases (the plots for the peak height are included as Figure S1).

The plots in Figure 8 have two notable features. The first is the time-delay in Stage III before the monoclinic phase emerges. Moreover, initially, the (002) peak from the monoclinic phase fluctuates with time before yielding a steady rise in its intensity, with a complementary reduction in the (111) peak from the cubic phase. The second feature of these plots is that the monoclinic phase dissolves, and the complementary cubic phase recovers, in just a few seconds, when the current is stopped.

It has been reported that excess oxygen anion vacancies could be induced during flash sintering of oxide ceramics.^{3,6,22} The excess oxygen vacancies have been postulated to stabilize the cubic phase in a matrix of the tetragonal phase.²³ However, the present study shows cubic to monoclinic phase transformation. This result may have arisen from the different chemistry. In the present work we use the cubic phase of zirconia whereas the earlier work started

with the tetragonal phase. It is also possible that that mechanical constraint imposed by the surrounding MgO-Al₂O₃ matrix may have stabilized the monoclinic phase.^{24,25}

Similar results have been reported with 3YSZ where time-dependent emergence of the cubic phase in tetragonal zirconia.⁸ Similarly, in titania fluctuation in the intensity of diffraction peaks was seen during Stage III.⁹ Both experiments were carried out at synchrotrons (APS and NSLS-II).

3.4 | Measurements and estimates of the specimen temperature

We report the measurement of the specimen temperature from the Pt standard, and the estimate of the specimen temperature from the BBR model prescribed by Eq. 2. The objective is to elicit information about the change in the emissivity of the specimen as it transforms into spinel.

The calibration curves for the Pt standard were obtained by comparing the peak shifts, measured by increasing the furnace temperature, without the presence of electric field, using the handbook data for thermal expansion. The peak shifts were related to the data for thermal expansion by following equation:⁸

$$\frac{\Delta a}{a_0} = \frac{\sin(\theta_{hkl,0})}{\sin(\theta_{hkl})} - 1 \quad (3)$$

where $\Delta a/a_0$ is lattice parameter change and $\theta_{hkl,0}$ and θ_{hkl} are peak position at room temperature and high temperature. We used two platinum peaks, (111) and (200) to measure temperature from peak shift. The calibration curves obtained in this way are given in Figure 9.

It is to be noted that the radiant furnace used in the present experiments can have a discrepancy between the thermocouple and the actual specimen temperature. This occurs because the thermocouple could not be placed very close to the specimen since it would have obstructed the path of the X-ray beam. Thus, in the present experiments, the furnace temperature was set at 900°C, but specimen temperature calculated from platinum standard was 975°C. We have used this latter value for the BBR calculation.

The estimate from the BBR model (Equation 2) requires the value for the emissivity. From literature spinel has a lower emissivity than zirconia. While the emissivity for zirconia is ~0.9, the emissivity of spinel at 1000 K is 0.27.²⁶ In a recent study, Kok et al¹² used rule of mixture to find optimum emissivity of a composite of spinel and zirconia. Emissivity of spinel was extrapolated to 0.19 at 1600°C from literature value, and emissivity of zirconia was set

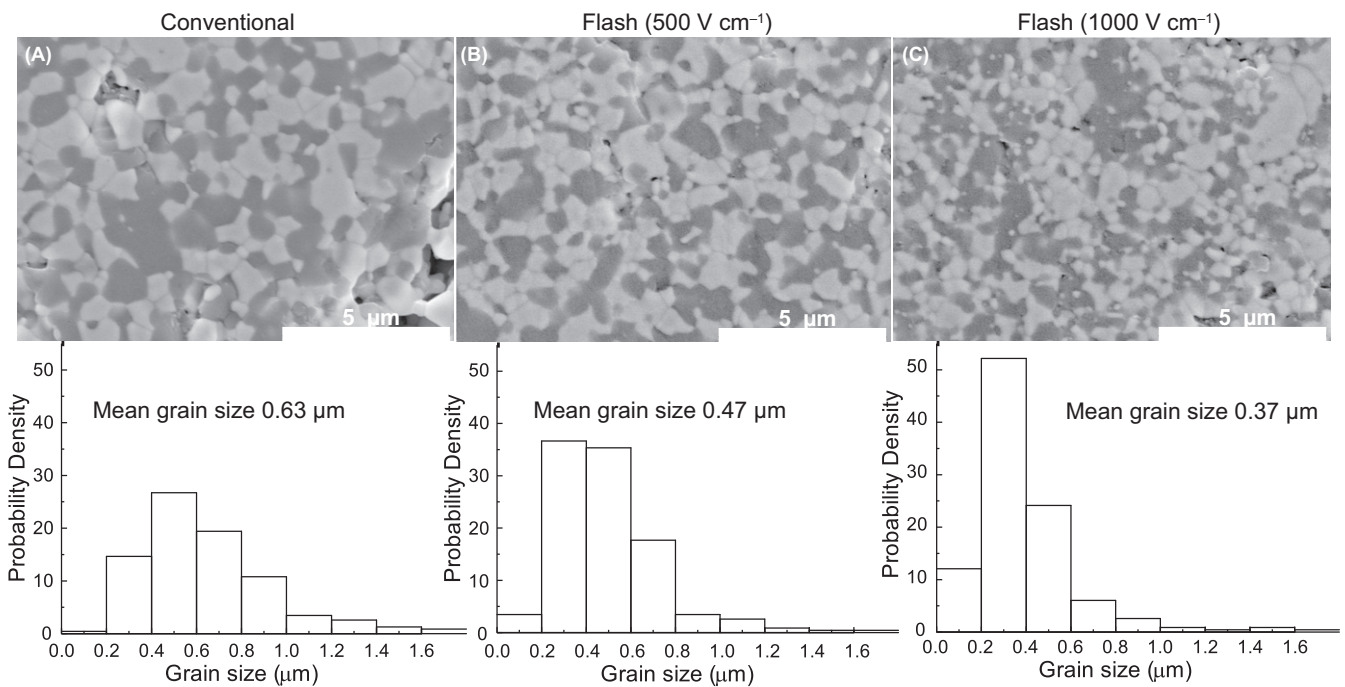


FIGURE 4 Microstructure and grain size distribution of 8YSZ-MgO-Al₂O₃ composite (A) conventionally sintered at 1550°C for 2 h, (B) flash sintered at 500 V/cm and (C) 1000 V/cm

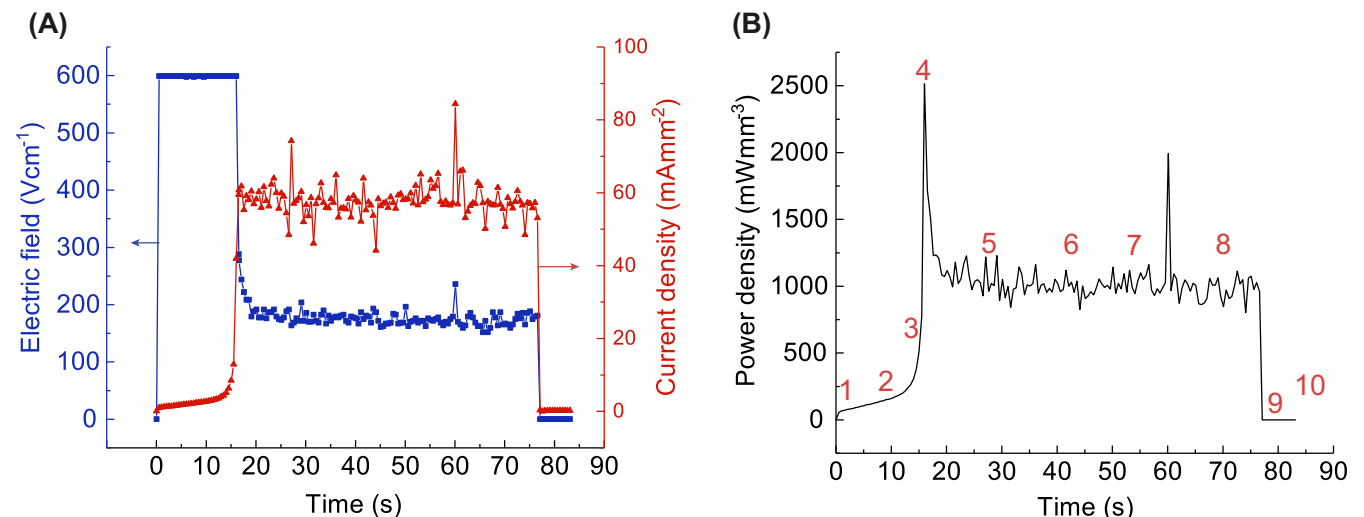


FIGURE 5 A, The electric field and current density curves, and B, power density curve of synchrotron experiments under electric field of 600 V/cm and current density of 60 mA/mm² [Color figure can be viewed at wileyonlinelibrary.com]

equal 0.9.²⁶ These values when combined by the rule-of-mixtures gave good agreement between the BBR estimate and the in situ measurement.¹²

In the present study, rule of mixtures gave an emissivity value of 0.57. The data for the specimen temperature from the platinum standard is plotted along with the BBR-model prediction for emissivity values of 0.6, 0.7, and 0.8 in Figure 10. A reasonable agreement is obtained for emissivity in the range of 0.6–0.7, which is somewhat higher than

calculated from the rule of mixtures. The difference may be due to the presence of minor amount of residual alumina, which has a higher emissivity than spinel (0.48 at 1500°C).²⁷

4 | DISCUSSION

This study has yielded three results,

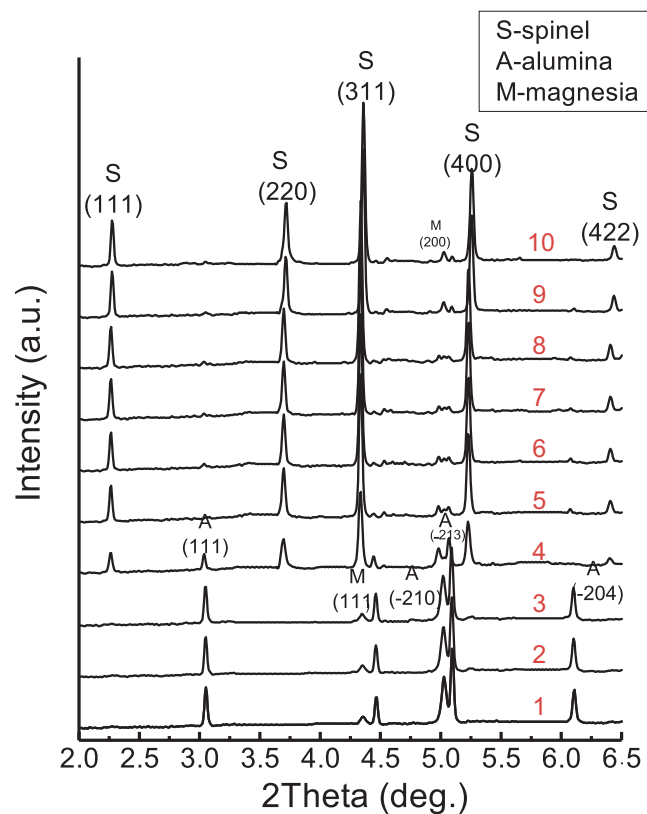


FIGURE 6 In situ XRD patterns of alumina, magnesia, and spinel, corresponding points from 1 to 10 in Figure 5B [Color figure can be viewed at wileyonlinelibrary.com]

- The addition of zirconia can catalyze flash sintering of ceramics which are intrinsically insulating and therefore, difficult to flash by themselves,
- Sintering and phase transformation of magnesia and alumina into spinel occurs simultaneously, in Stage II, and,
- Non-equilibrium phase transformation of zirconia, from cubic to monoclinic phase, occurs during Stage III, but which reverts to the original cubic phase when the current flowing through the specimen is stopped.

The influence of zirconia on instigating flash in alumina and magnesia, is likely related to the effect of zirconia on the overall electrical conductivity. There is growing evidence that the onset of the flash, marked by the cusp in the abrupt rise in the power dissipation, occurs within a narrow range of power density. Therefore, we can say that the effect of zirconia is related to its effect on the electrical conductivity of the composite.¹⁸ In summary, the addition of high conductivity zirconia to much more insulating ceramics (alumina and magnesia) catalyzes the onset of the flash.

The power cusp discussed above implies the necessity of Joule heating in instigating the flash. However, it does

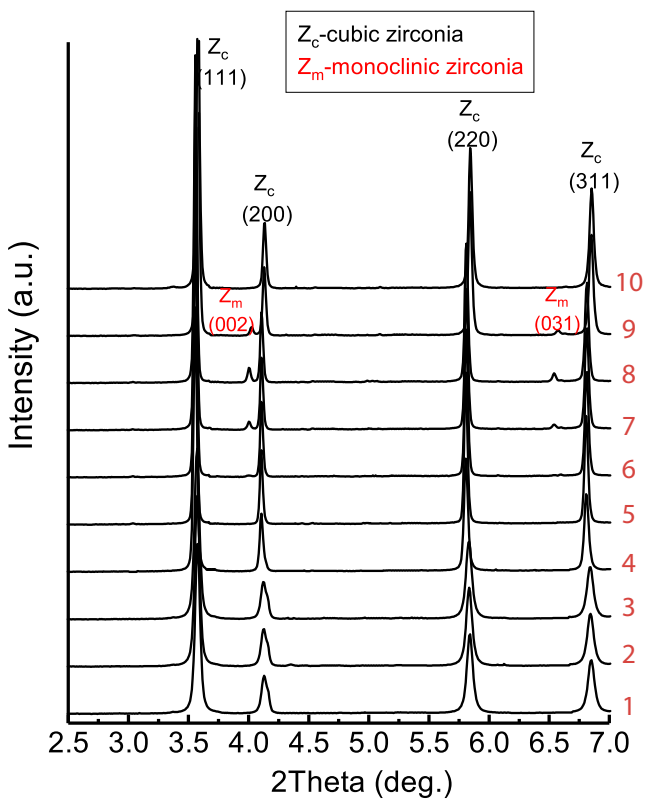


FIGURE 7 In situ XRD patterns of zirconia corresponding points from 1 to 10 in Figure 5B. Note that new peaks (Monoclinic (002) and (031)) developed during of Stage III. The new peaks dissolve when the field is turned off [Color figure can be viewed at wileyonlinelibrary.com]

not imply that it must lead to thermal runaway. Indeed the flash is preceded by an incubation time where the specimen conductivity rises gradually until it reaches a critical

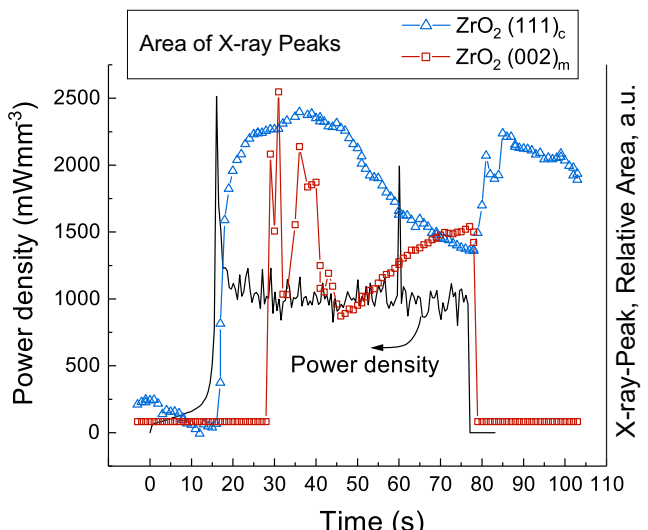


FIGURE 8 Power dissipation curve, synchronized with the change in the area under the diffraction peaks from cubic ZrO_2 (111) and monoclinic ZrO_2 (002), at a current density of 60 mA/mm^2 [Color figure can be viewed at wileyonlinelibrary.com]

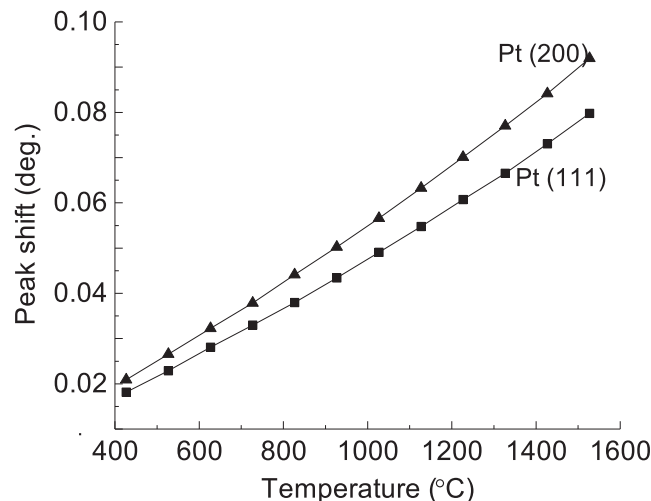


FIGURE 9 Specimen temperature calibration curve from shifts in the peaks from platinum (without the application of electric field). Peak shifts of (111) and (200) were calculated from room temperature position, which were 4.72 and 5.45°, respectively. Coefficient of thermal expansion of platinum was used to calibrate the sample temperature

value before the onset of the flash.¹⁸ Closed form analysis has shown that in most instances after the power density cusp, the temperature would reach a steady-state value.¹⁸ Indeed numerical analysis also shows that the rate of cooling from black body radiation exceeds the electrical rate of heating when the furnace temperature is below 1339 K, in the case of flash in 3YSZ (for example see Figure 4 in Ref.²⁸). If BBR cooling is greater than the power dissipation the specimen is expected to reach a steady state in temperature, not indefinite thermal runaway.

More generally, the thermal runaway idea depends greatly on the activation energy for the conductivity since the change in the conductivity with temperature is a critical feature of the indefinite runaway concept. However, a wide range of ceramics, which include semiconductors, electronic conductors and ionic conductors, having an immensely wide range of activation energies for their conductivity, have been shown to behave in a similar manner, with a similar power density at the cusp of the flash.¹⁸

The present work shows that sintering and phase transformation of magnesia and alumina into spinel can occur simultaneously during Stage II of the flash experiment. Both of these phenomena are diffusion controlled, but with a difference. Sintering requires chemical diffusion while phase transformation not necessarily. In summary, it remains far from clear how sintering and phase transformations are coupled, in time.

In situ flash-sintering experiments with tetragonal zirconia (3YSZ) have shown the emergence of a non-equilibrium pseudo-cubic phase when the specimen is held in

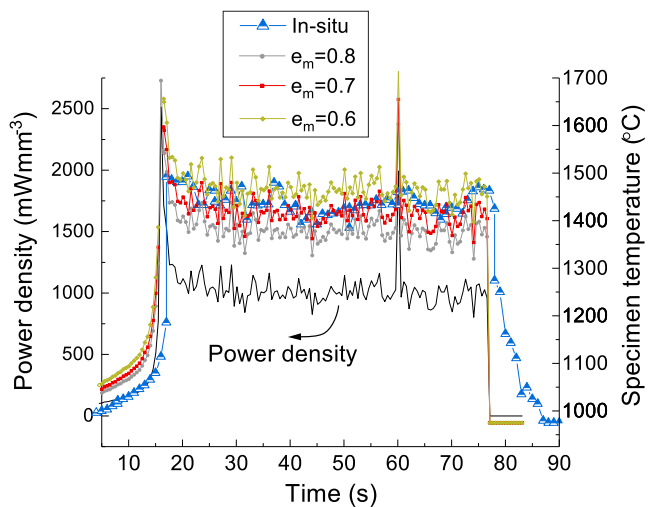


FIGURE 10 Power density and specimen temperature estimation from in-situ measurements and black body radiation with various emissivities [Color figure can be viewed at wileyonlinelibrary.com]

Stage III.⁸ In present work we started with the cubic phase which is stabilized by 8YSZ. We show that it partly transforms, apparently, to the monoclinic phase, which reverts to the cubic phase when the field is turned off. Like in Ref⁸ the transformation is time dependent. The transformation of the tetragonal 3YSZ into the cubic phase could be explained in terms of the high oxygen vacancy concentrations induced by the flash. It is possible that the cubic to monoclinic transformation is also related to the generation of defects during flash. The mechanical constraint from the surrounding spinel matrix may also have played a role.³⁰

In any event, there is increasing evidence that unusual concentrations of defects generated by flash may lead to unpredictable effects such as phase transformations which are not predicted by the phase diagrams.^{8–10,15,31}

5 | CONCLUSIONS

Reactive flash sintering of MgO and Al₂O₃ into single phase spinel has been studied. 8YSZ was added for inducing flash sintering by increasing the conductivity. Transformation of spinel occurred in Stage II within a few seconds, along with densification of spinel. In Stage III, cubic zirconia partly transformed into monoclinic phase, which extinguished when power was off. Specimen temperature was measured by in situ experiments at NSLS-II.

During revision we have come across a new paper^{32,33} which highlights the role of the conductivity of the specimen in instigating the flash. In the present work we show that at a given applied field the addition of zirconia moves the flash temperature to lower values; however the flash occurs at the temperature when the

specimen reaches the same value of conductivity. In reference³² the conductivity of strontium titanate was varied by doping with Fe and by changing the oxygen activity; at a given value of the electric field the flash occurred at the temperature where the specific conductivity for these specimens reached the same value.

ACKNOWLEDGMENTS

This research was supported by a grant, W911NF-16-1-0200, from the Army Research Office, under the direction of Dr. Michael Bakas, and by Office of Science of the Department of Energy, Grant/Award Number: DE-AC02-98CH10886. It is a pleasure to acknowledge Prof. Pankaj Sarin of Oklahoma State University for providing us with the quadruple lamp furnace and his expertise in its use. BY expresses her thanks to Heejung Jung, University of Colorado Boulder, for help in MATLAB analysis of the diffraction data. This research used 28ID-2 (XPD) beamline of the National Synchrotron Light Source II, a US Department of Energy (DOE) Office of Science User Facility operated for the DOE Office of Science by Brookhaven National Laboratory under Contract No. DE-SC0012704.

ORCID

Bola Yoon  <http://orcid.org/0000-0002-6087-5373>
Sanjit Ghose  <http://orcid.org/0000-0003-0245-8560>
Rishi Raj  <http://orcid.org/0000-0001-8556-9797>

REFERENCES

1. Cologna M, Rashkova B, Raj R. Flash sintering of nanograin zirconia in <5 s at 850°C. *J Am Ceram Soc.* 2010;93:3556–9.
2. Jha SK, Raj R. The effect of electric field on sintering and electrical conductivity of titania. *J Am Ceram Soc.* 2014;97:527–34.
3. Yoshida H, Sakka Y, Yamamoto T, Lebrun J-M, Raj R. Densification behaviour and microstructural development in undoped yttria prepared by flash-sintering. *J Eur Ceram Soc.* 2014;34: 991–1000.
4. Cologna M, Francis JSC, Raj R. Field assisted and flash sintering of alumina and its relationship to conductivity and MgO-doping. *J Eur Ceram Soc.* 2011;31:2827–37.
5. Charalambous H, Jha SK, Lay RT, Cabales A, Okasinski J, Tsakalakos T. Investigation of temperature approximation methods during flash sintering of ZnO. *Ceram Int.* 2018;44:6162–9.
6. Yoshida H, Biswas P, Johnson R, Mohan MK. Flash-sintering of magnesium aluminate spinel ($MgAl_2O_4$) ceramics. *J Am Ceram Soc.* 2017;100:554–62.
7. Gil-González E, Perejón A, Sánchez-Jiménez PE, Sayagués MJ, Raj R, Pérez-Maqueda LA. Phase-pure $BiFeO_3$ produced by reaction flash-sintering of Bi_2O_3 and Fe_2O_3 . *J Mater Chem A.* 2018;6:5356–66.
8. Lebrun J-M, Morrissey TG, Francis JSC, Seymour KC, Kriven WM, Raj R. Emergence and extinction of a new phase during on-off experiments related to flash sintering of 3YSZ. *J Am Ceram Soc.* 2015;98:1493–7.
9. Jha SK, Lebrun JM, Seymour KC, Kriven WM, Raj R. Electric field induced texture in titania during experiments related to flash sintering. *J Eur Ceram Soc.* 2016;36:257–61.
10. Jha SK, Lebrun JM, Raj R. Phase transformation in the alumina-titania system during flash sintering experiments. *J Eur Ceram Soc.* 2016;36:733–9.
11. Kok D, Jha SK, Raj R, Mecartney ML. Flash sintering of a three-phase alumina, spinel, and yttria-stabilized zirconia composite. *J Am Ceram Soc.* 2017;100:3262–8.
12. Kok D, Yadav D, Sortino E, McCormack SJ, Tseng K-P, Kriven WM, et al. α -Alumina and spinel react into single phase high-alumina spinel in < 3 seconds during flash sintering. *J Am Ceram Soc.* In press 2018.
13. Francis JSC, Raj R. Influence of the field and the current limit on flash sintering at isothermal furnace temperatures. *J Am Ceram Soc.* 2013;96:2754–8.
14. Shi X, Ghose S, Dooryhee E. Performance calculations of the X-ray powder diffraction beamline at NSLS-II. *J Synchrotron Radiat.* 2013;20:234–42.
15. Yoon B, Yadav D, Raj R, Sortino E, Ghose S, Sarin P, et al. Measurement of O and Ti atom displacements in TiO_2 during flash sintering experiments. *J Am Ceram Soc.* 2018;101:1811–7.
16. Hammersley AP, Svensson SO, Thompson A, Graafsma H, Kvick Å, Moy JP. Calibration and correction of distortions in two-dimensional detector systems. *Rev Sci Instrum.* 1995;66:2729–33.
17. Hahn TA, Kirby RK. Thermal expansion of platinum from 293 to 1900 K. *AIP Conf Proc.* 1972;3:87–95.
18. Raj R. Analysis of the power density at the onset of flash sintering. *J Am Ceram Soc.* 2016;99:3226–32.
19. Ganesh I, Olhero SM, Rebelo AH, Ferreira JMF. Formation and densification behavior of $MgAl_2O_4$ spinel: the influence of processing parameters. *J Am Ceram Soc.* 2008;91:1905–11.
20. Naik KS, Sglavo VM, Raj R. Field assisted sintering of ceramic constituted by alumina and yttria stabilized zirconia. *J Eur Ceram Soc.* 2014;34:2435–42.
21. Francis JSC, Cologna M, Raj R. Particle size effects in flash sintering. *J Eur Ceram Soc.* 2012;32:3129–36.
22. Morisaki N, Yoshida H, Matsui K, Tokunaga T, Sasaki K, Yamamoto T. Synthesis of zirconium oxynitride in air under DC electric fields. *Appl Phys Lett.* 2016;109:083104.
23. Asgarani MK, Saidi A, Abbasi MH. Role of oxygen vacancy and grain boundary energy in stability of tetragonal and cubic pure zirconia powders. *Powder Metall.* 2011;54:127–32.
24. Schmauder S, Schubert H. Significance of internal stresses for the martensitic transformation in yttria-stabilized tetragonal zirconia polycrystals during degradation. *J Am Ceram Soc.* 1986;69:534–40.
25. Hannink RHJ, Kelly PM, Muddle BC. Transformation toughening in zirconia-containing ceramics. *J Am Ceram Soc.* 2000;83:461–87.
26. Palik ED. *Handbook of optical constants of solids*. New York, NY: Academic Press; 1991.
27. Blair GR. Determination of spectral emissivity of ceramic bodies at elevated temperatures. *J Am Ceram Soc.* 1960;43:197–203.
28. Raj R. Joule heating during flash-sintering. *J Eur Ceram Soc.* 2012;32:2293–301.

29. Bratton RJ. Initial sintering kinetics of MgAl₂O₄. *J Am Ceram Soc.* 1969;52:417–9.
30. Ganesh I. A review on magnesium aluminate (MgAl₂O₄) spinel: synthesis, processing and applications. *Int Mater Rev.* 2013;58:63–112.
31. Lebrun J-M, Hellberg CS, Jha SK, Kriven WM, Steveson A, Seymour KC, et al. In-situ measurements of lattice expansion related to defect generation during flash sintering. *J Am Ceram Soc.* 2017;100:4965–70.
32. Ze'ev BM, Neta S, Yoed T. Recent advances in mechanism research and methods for electric-field-assisted sintering of ceramics. *Adv Mater.* In press 2018.
33. Shomrat N, Baltianski S, Dor E, Tsur Y. The influence of doping on flash sintering conditions in SrTi_{1-x}Fe_xO_{3-δ}. *J Eur Ceram Soc.* 2017;37:179–88.

SUPPORTING INFORMATION

Additional supporting information may be found online in the Supporting Information section at the end of the article.

How to cite this article: Yoon B, Yadav D, Ghose S, Raj R. Reactive flash sintering: MgO and α -Al₂O₃ transform and sinter into single-phase polycrystals of MgAl₂O₄. *J Am Ceram Soc.* 2019;102:2294–2303.

<https://doi.org/10.1111/jace.15974>